

## **Segmentation and Detection of Extended Structures in Low Frequency Astronomical Surveys using Hybrid Wavelet Decomposition**

Marta Peracaula,<sup>1</sup> Xavier Lladó,<sup>1</sup> Jordi Freixenet,<sup>1</sup> Arnau Oliver,<sup>1</sup> Albert Torrent,<sup>1</sup> Josep M. Paredes,<sup>2</sup> and Josep Martí<sup>3</sup>

<sup>1</sup>*Institut d'Informàtica i Aplicacions, Universitat de Girona, Spain*

<sup>2</sup>*Departament d'Astronomia i Meteorologia, Facultat de Física, Universitat de Barcelona, Spain*

<sup>3</sup>*Departamento de Física, Escuela Politécnica Superior, Universidad de Jaén, Spain*

**Abstract.** The morphological complexity of extended real structures (such as SNRs, HII regions, bow shocks, etc.), and their wide variety in scale and surface brightness make their automatic detection and segmentation in large surveys a difficult task. We propose in this paper a segmentation method based on applying wavelet decomposition in the residual thresholded images. This strategy avoids the artifacts produced by strong sources in a straight wavelet decomposition. Our method successfully segments extended structures at different scales and therefore is suitable for further morphological analysis and object recognition processes. Results using images from radio and infrared wavelengths surveys show the validity of our approach.

### **1. Motivation and Objectives**

Large surveys reveal thousands of low spatial frequency objects, shown at different intensity scales. When imaging rich areas in the interstellar medium, many of the compact sources overlap with objects associated to extended, morphologically complex real structures, such as SNRs, HII regions, bow shocks, etc. The wide variety in spacial scale and surface brightness of these objects make their automatic detection and segmentation a difficult task.

To illustrate these facts, we use in this paper the image corresponding to the high galactic longitude end of the Phase I Canadian Galactic Plane Survey (CGPS hereafter, see Taylor et al. 2003). Figure 1 shows, on the top, the image composition corresponding to mosaics V1, V2, W1, W2, X1, X2, Y1 and Y2 of the CGPS 1420 MHz, continuum. We have eliminated 0.1% of the intensity outliers in order to visualize some dozens of sources. Nevertheless, the data corresponding to these mosaics contain thousands of objects, as it is illustrated when we display the sub-image contained in the red square at different intensity scales. On the bottom left of the figure we show the sub-image with 2% of the outliers eliminated, whereas on the right 5% of them have been removed. In addition to a great number of compact sources, several extended structures and their surrounding emission have appeared (the zoomed area contains Lynds Bright Nebula 679).

In previous work we focused our attention on the performance of techniques suitable for the detection of faint compact objects (see for example Peracaula et al. 2008). In the present work we focus on the automatic detection of extended and irregular structures for further cataloguing and morphological analysis. In this context, wavelet image decomposition has been proven as a tool that can detect and separate objects represented at different spatial frequencies. However, the high dynamic range in intensity of this kind of image diminishes the performance

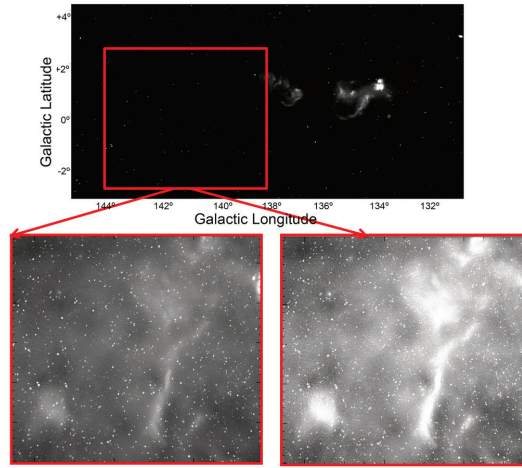


Figure 1. Top: Contrast stretched (0.1% outliers eliminated) image corresponding to mosaics V1, V2, W1, W2, X1, X2, Y1 and Y2 of Phase I CGPS at 1420 MHz, continuum. Bottom: Zoomed area around Lynds Bright Nebula 679, displayed with 2% of outliers eliminated (left) and 5% of outliers eliminated (right).

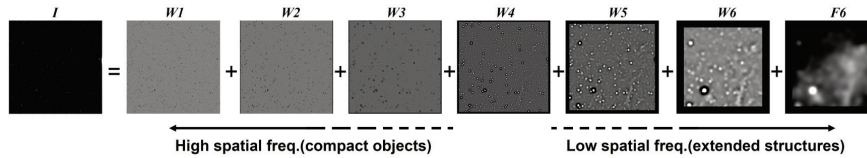


Figure 2. Wavelet decomposition of the sample image.

of the decomposition and a strategy to avoid this problem has to be applied, as we propose in the next sections.

## 2. Wavelet Decomposition Using the “à trous” Algorithm

Multiscale Vision Models (Bijaoui & Rué 1995) decompose an image in  $J$  scales or wavelet planes and segment independently each of the images representing a scale. In Figure 2 we use the image containing mosaics V1, V2, W1 and W2 of the CGPS at 1420 MHz (continuum), and decompose it in 6 scales plus the smoothed array using the “à trous” algorithm with a  $B_3$  filtering function (see for example Starck & Murtagh 1994, and references therein). As it can be seen, low index scales emphasize high spatial frequencies (which translates to compact objects and semi-compact in case of true signal). High index scales emphasize low spatial frequencies (in this case extended source structures).

Using this approach we encounter two major problems:

1. As shown in Figure 3, due to their high brightness, strong compact sources are not filtered out and show up in low spatial frequency planes,

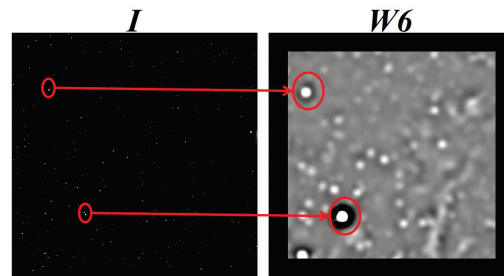


Figure 3. Strong compact sources (as the ones circled in the original image on the left), show up in low spatial frequency planes (right).

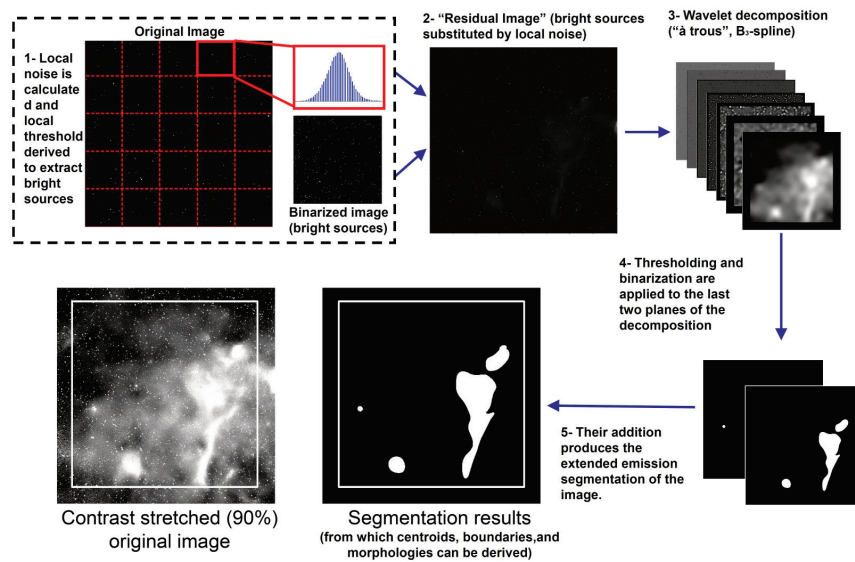


Figure 4. Graphical representation of our algorithm and visual comparison of the segmentation result with the contrast stretched image.

2. To keep the wavelet coefficient mean at zero, negative artifacts around these strong structures appear and pollute the entire image.

### 3. Our Approach

We propose to create an image where bright sources are substituted by local noise. Wavelet decomposition will then be applied to this new image in order to avoid the polluting effects of strong easily detectable sources. The algorithm we propose consists of the following steps:

1. We calculate local noise in the original image and derive a local threshold.

2. Pixels with intensity levels over the threshold are labeled and connected zones dilated in order to extract bright sources.
3. Two images are created: a “residual image” where bright sources have been substituted by local noise, and a binary image mask with the bright sources.
4. We apply a 6-scale Wavelet decomposition using the “à trous” algorithm and a  $B_3$ -spline filtering function to the “residual image”.
5. Local thresholding and binary masking is applied to the last scale and the smoothed array.
6. The addition of the last two binary planes of the decomposition produces the extended emission segmentation of the image.

In Figure 4 we show a graphical representation of the algorithm using the sample image. On the bottom left we show the contrast stretched sample image in order to compare it with the segmentation result.

**Acknowledgments.** The authors acknowledge support by DGI of the Spanish Ministerio de Educación y Ciencia (MEC) under grants AYA2007-68034-C03-01/02/03 and DPI2007-66796-C03-02, as well as partial support by the European Regional Development Fund (ERDF/FEDER). This research used the facilities of the Canadian Astronomy Data Center operated by the National Research Council of Canada with the support of the Canadian Space Agency. The research presented in this paper has used data from the Canadian Galactic Plane Survey a Canadian project with international partners supported by the Natural Sciences and Engineering Research Council.

## References

- Bijaoui, A., & Rué, F. 1995, *Signal Proc.*, 46, 345  
Peracaula, M., Freixenet, J., Martí, J., Martí, J., & Paredes, J. M. 2008, in *Astronomical Data Analysis Software and Systems XVII*, edited by R. W. Argyle, P. S. Bunclark, & J. R. Lewis (San Francisco, CA: ASP), vol. 394 of ASP Conf. Ser., 547  
Starck, J., & Murtagh, F. 1994, *A&A*, 288, 342  
Taylor, A. R., et al. 2003, *AJ*, 125, 3145